The Seybold REPORT

ISSN 1533-9211

DOI 10.17605/OSF.IO/HMJBN

THE CC-UNET MODEL OF HEAVY RAIN DETECTION IN MEDAN CITY FOR ANTICIPATING AQUACULTURE PRODUCTION LOSS

HUMUNTAL RUMAPEA[#*], MOHAMMAD ZARLIS[#], SYAHRIL EFENDY[#] and POLTAK SIHOMBING[#]

[#]Doctoral Study Program (S3) in Computer Science, Faculty of Computer Science and Information Technology, University of North Sumatra, Medan, North Sumatra, Indonesia.
[*]Corresponding author: hrumapea1608@gmail.com

Abstract

Harmful weather has a strong correlation with losses in aquaculture enterprises due to moderate to extreme floods. Such destruction greatly affects aquaculture productivity, lowering total production, production value, income, and Gross Regional Domestic Product. Convective clouds are highly correlated to rain. However, cloud detection as natural disaster mitigation is a challenging task to work on at times. Therefore, artificial intelligence as part of computer science is needed to help simplify the complexity of natural disaster mitigation. By employing secondary data on regional development parameters 2010-21 obtained from the Central Statistics Agency of Medan City 2022, such as Gross Regional Domestic Product (GRDP), Poverty Rate (POV), Human Development Index (HDI), and Aquaculture Production (AP), the present study desired to find the causality relationship between those variables through the Autoregressive Distributed Lag (ARDL) Model on EViews 9.0. Besides, in solving the complexities of cloud detection, this study used a predictive-analytic classification of the CC-Unet model based on deep learning to improve the classification results of convective clouds by taking the advantages of Himawari 8 satellite image data collected on 13 May 2021 and 30 October 2021. The present study found that if the local government in Medan City could increase GRDP and aquaculture production by 1% while also protecting the aquaculture sector from floods, poverty could be reduced by 0.094561% and 0.817079% respectively. In terms of cloud detection, the CC-Unet model in this study has a better accuracy of 97.29% compared to the U-Net model (94.17%). Shrimp farming businesses in Medan City, especially Aur Village, to prevent losses against their shrimp production, can use the prediction of flooding. Consequently, poverty could be eliminated.

Subjects: Computer Science; Macroeconomics; Statistics; Disaster Mitigation.

Keywords: Convective cloud, CC-Unet, disaster mitigation, poverty.

1. INTRODUCTION

The phenomenon of inundation due to non-proportional absorption of soil is one of the main causes of flood catastrophes that must be addressed immediately as it has had many systemic adverse effects on human life in rural and urban areas. Although rain is one of the key factors in balancing the earth's hydrography (Prabawadhani et al., 2016), urban areas which are generally low-lying regions often experience flooding due to overflowing rivers that cannot accommodate high precipitation. Such events have a negative impact on human activities holistically (Harisdani & Lindarto, 2018). Medan, as one of the largest provincial capitals in Indonesia, is the center of the economy and government in North Sumatra which continues to improve in constructing modern and livable urban planning. Unfortunately, flooding, climate change, and the difficulty in predicting rain are inevitable for this city.

The Seybold REPORT
ISSN 1533-9211
DOI 10.17605/OSF.IO/HMJBN

According to several researchers (Posthumus et al., 2008; Surminski & Eldridge, 2017), flooding is one of the disasters with the highest level of destruction in all aspects. The damage caused is also often unexpected because it can destroy various domains of people's lives. A study by Molle et al., (2010) found that one of the most vulnerable sectors due to floods was aquaculture. The sensitivity of this sector to floods is because the media in aquaculture does depend on water quality. Poor water quality due to floods directly harms aquaculture businesses and inconveniences all actors involved. Pond fisheries in the aquaculture industry are highly dependent on the hydrological cycle, and loads of dirty suspended sediments are definitely unfavorable for shrimp culture's water circulation (Anbumozhi et al., 2001; Mushtaq et al., 2006; Mushtaq et al., 2007). In addition to the polluted water that can inundate pond areas, according to several researchers (Toth et al., 1982; Schlosser, 1985; Harvey, 1987; Sato, 2006), sudden environmental changes that cause a decrease in water quality due to flooding can cause mass death against aquaculture outcomes. During the rainy season, Medan is always flooded where economic reasons through land development and conversion are the biggest contributors to this problem (Tarigan et al., 2017).

Over the past few decades, there has been an evolution of learning from machine learning to deeper learning in addressing various problems of prediction, detection, and mitigation of natural disasters in Indonesia. Therefore, learning related to methods that progress to be more appropriate to provide solutions to disaster mitigation is urgently needed (Ackerman et al., 1998; Baker & Peter, 2008; She et al., 2020; Liu et al., 2021).

Deep learning is an important element of data science that covers statistics and predictive modeling to make it easier for scientists to collect, analyze, and interpret large amounts of data. In addition, this technique can perform automation processes to perform analysis and predictions. In contrast to traditional machine learning which uses a linear hierarchy, deep learning algorithms are designed in a non-linear manner that involves many layers. In detecting convective clouds, the present study employed the Convolution Neural Network (CNN) which is one class of artificial neural networks (Frey et al., 2008; Baum et al., 2012; Bai et al., 2016; Bessho et al., 2016; Chen et al., 2018; Gomis-Cebolla et al., 2020) and used satellite images obtained via the Himawari 8 Satellite.

Even though the regional government has carried out several plans to control flooding, the implementation is lacking which causes waterlogging still in records with the worst incident occurring on December 4, 2020; documented as the worst flood in the last 20 years (Rahmawati, 2020). The flood catastrophe is certainly damaging water quality and causes losses in businesses that depend on the hydrological cycle for their activities. Therefore, the present study investigates the relationship among regional economic development parameters that plays a role in the socio-economic development of the aquaculture community.

Furthermore, this study will also discuss how to embrace the regional development parameters from the computer science perspective through better convective cloud forecasts that can be used as a flood early warning system. It is hoped that the government can understand that floods can damage the economy of the aquaculture community in Medan City, and good disaster

The Seybold REPORT
ISSN 1533-9211
DOI 10.17605/OSF.IO/HMJBN

detection needs to be implemented immediately so that mitigation can also be executed optimally.

2. MATERIALS AND METHODS

2.1 Econometrics Cointegration

In finding out the relationship among all socio-economic characteristics and how this relationship can be embraced through a better forecast of flood disasters, this study used secondary data on regional development parameters 2010-21 obtained from the Central Statistics Agency for Medan City 2022, consisting of Gross Regional Domestic Product (GRDP), Poverty Rate (POV), Human Development Index (HDI), and Aquaculture Production (AP). Model processing began by carrying out the Augmented Dickey-Fuller unit root test (Dickey & Fuller, 1979) to check the stationarity of the data. The main requirement for the Autoregressive Distributed Lag (ARDL) Model on EViews 9.0 to be carried out is that all variables must be at the order level (0) or order 1 (first difference). The ARDL model cannot be applied and causality analysis cannot be carried out if the main conditions are not met.

Determining the optimum lag as the next step was carried out by adopting the Akaike Information Criterion (AIC) through Vector Autoregression Estimates (VAR) for all variables. The best way to choose the optimal lag is to look at the smallest AIC value. Later, the optimum lag value was used when running ARDL Cointegrating and Long Run Form with the formula below:

$$\Delta \ln GRDP_t = \alpha_\circ + \alpha_T T + \alpha_{GRDP} \ln GRDP_{t-1} + \alpha_{POV} \ln POV_{t-1} + \alpha_{AQP} \ln AP_{t-1} + \alpha_{HDI} \ln HDI_{t-1} + \sum_{i=1}^{p} \alpha_i \Delta \ln GRDP_{t-i} + \sum_{j=0}^{q} \alpha_j \Delta \ln POV_{t-j} + \sum_{k=0}^{l} \alpha_K \Delta \ln AP_{t-k} + \sum_{l=0}^{m} \alpha_l \Delta \ln HDI_{t-l} + \varepsilon_t \quad \ldots\ldots (1)$$

$$\Delta \ln POV_t = \alpha_\circ + \alpha_T T + \alpha_{PV} \ln POV_{t-1} + \alpha_{GRDP} \ln GRDP_{t-1} + \alpha_{AP} \ln AP_{t-1} + \alpha_{HDI} \ln HDI_{t-1} + \sum_{i=1}^{p} \alpha_i \Delta \ln POV_{t-i} + \sum_{j=0}^{q} \alpha_j \Delta \ln GRDP_{t-j} + \sum_{k=0}^{l} \alpha_K \Delta \ln AP_{t-k} + \sum_{l=0}^{m} \alpha_l \Delta \ln HDI_{t-l} + \varepsilon_t \quad \ldots\ldots.. (2)$$

$$\Delta \ln AP_t = \alpha_\circ + \alpha_T T + \alpha_{AP} \ln AP_{t-1} + \alpha_{GRDP} \ln GRDP_{t-1} + \alpha_{POV} \ln POV_{t-1} + \alpha_{HDI} \ln HDI_{t-1} + \sum_{i=1}^{p} \alpha_i \Delta \ln AP_{t-i} + \sum_{j=0}^{q} \alpha_j \Delta \ln GRDP_{t-j} + \sum_{k=0}^{l} \alpha_K \Delta \ln POV_{t-k} + \sum_{l=0}^{m} \alpha_l \Delta \ln HDI_{t-l} + \varepsilon_t \quad \ldots\ldots.. (3)$$

$$\Delta \ln HDI_t = \alpha_\circ + \alpha_T T + \alpha_{HDI} \ln HDI_{t-1} + \alpha_{GRDP} \ln GRDP_{t-1} + \alpha_{POV} \ln POV_{t-1} + \alpha_{AP} \ln AP_{t-1} + \sum_{i=1}^{p} \alpha_i \Delta \ln HDI_{t-i} + \sum_{j=0}^{q} \alpha_j \Delta \ln GRDP_{t-j} + \sum_{k=0}^{l} \alpha_K \Delta \ln POV_{t-k} + \sum_{l=0}^{m} \alpha_l \Delta \ln AP_{t-l} + \varepsilon_t \quad \ldots\ldots.. (4)$$

Causality can explain how one variable affects the rest variables. Proving causality between variables can be done in a more detailed way by knowing if long-term cointegration existed. The cointegrating results of ARDL Cointegrating and Long Run Form were compared with Upper Critical Bound (UCB) and Lower Critical Bound (LCB) as suggested by Pesaran et al., (2001):

The Seybold REPORT
ISSN 1533-9211
DOI 10.17605/OSF.IO/HMJBN

- F-Statistics > UCB= cointegration;
- F-Statistics < LCB = no cointegration;
- LCB < F-statistics < UCB = undefined.

The Vector Error Correction Model (VECM) to look for further causal relationships was carried out because cointegration was found with the following equation:

$$AP_t = \alpha_{o1} + \sum_{i=1}^{l} \alpha_1 \Delta \ln AP_{t-i} + \sum_{j=1}^{m} \alpha_2 \Delta \ln GRDP_{t-j} + \sum_{k=1}^{n} \alpha_3 \Delta \ln POV_{t-k} + \sum_{l=1}^{o} \alpha_4 \Delta \ln HDI_{t-l} + \lambda_1 ECT_{t-1} + \varepsilon_t \quad \text{..... (5)}$$

Ln GRDP: Gross Regional Domestic Product;

Ln POV: Poverty;

Ln AP: Aquaculture Production;

Ln HDI: Human Development Index;

T: Trend variables in the ARDL Model and Bound Tests;

$\alpha_0, \alpha_{1,} \alpha_{2,} \alpha_{3,} \alpha_{4,}$: Drift components;

α_T: Time trends;

λECT: Vector of the Error Correction term; and

ε_t: White noise error.

To find out how one variable affects other variables in the long term, this study used Hsiao-Granger (Kollias et al., 2004).

2.2 The Convolution Neural Network

The convolution neural network (CNN)-based image segmentation consists of two approaches: region-based semantic segmentation (RBSS) and Fully Convolution Network-based Semantic Segmentation (FCNBSS) (Guo et al., 2018; Hao et al., 2020). Image segmentation using the first approach is done by breaking the image into smaller parts through a complicated process, especially in complex images. In contrast, segmentation in the second approach is directly based on image pixels without extracting image features. Therefore, the analysis in image segmentation is more directed at developing FCNBSS-based models (Minaee et al., 2021).

Furthermore, the development of the FCNBSS-based model has two approach models: SegNet (Badrinarayanan et al., 2017) and U-Net (Ronneberger et al., 2015). Both models have been successfully applied to cloud image segmentation. Besides, there are other models related to cloud image segmentation, such as CD-Unet (Hu et al., 2021), Refined U-Net model (Jiao et al., 2020), and SegCloud (Xie et al., 2020).

According to the literature studies (Lou et al., 2021; Liu et al., 2022), the U-Net-based model is more effective than SegNet because its model can distinguish the scale of image features even for small data. However, when faced with complex images, the model often fails to give

The Seybold REPORT
ISSN 1533-9211
DOI 10.17605/OSF.IO/HMJBN

satisfactory results due to background image factors that can affect the segmentation results. The background image factor is represented by the presence of disturbing objects that can affect the final result of cloud image segmentation such as natural phenomena, buildings, and other physical factors which are problems that often emerge. Based on these considerations, it is necessary to make improvements so that the U-Net model can capture image segments without interference. Improvements to the U-Net model are expected to increase its ability to minimize the noise in image data, especially when it comes to the cloud readings.

In this study, residuals were minimized by doubling the U-Net channel into two channels which were applied to the main segment extraction and residuals by adopting previous studies in removing image residues using multiple channels (Lou et al., 2021) and double branching (Liu et al., 2022). Both previous researchers have successfully applied the dual-channel principle in overcoming image residues. Therefore, based on the described background, this study built the CC-Unet model, a deep learning-based technique to detect convective clouds (CC) by improving the performance of the previous U-Net for detecting the type of cumulonimbus cloud sourced from the satellite (Mohanty et al., 2020). The prediction results will then be used as a flood early warning system.

2.3 U-NET Architecture

The U-Net architecture introduced by Ronneberger et al., (2015) is one of the first convolution networks specifically designed for biomedical image analysis. This architecture is a derived FCN network that aims to address two domain-specific problems in medical image segmentation to produce competitive segmentation results despite relatively small training data (Ito & Ino, 2018; Pan et al., 2020). Furthermore, a large data set with a fully connected Feed-forward CNN layer was usually used to analyze multiple parameters. Therefore, this type of model has the advantage of being able to learn with little information from multiple samples, for example, in medical image segmentation where the model needs to maximize learning from each sample.

Technically speaking, cloud image segmentation needs to maximize the information learned from any given instance. Encoder-decoder architectures such as U-Net have proven to be more effective, even with small datasets due to the ability of up-convolution circuits to replace the fully connected layer on the decoder even if there are still significantly fewer learnable parameters than the fully connected layer (Yu & Koltun, 2016; Kong et al., 2022). The other problem that the U-Net architecture addresses is capturing context accurately and localizing the lesion at different scales and resolutions.

ISSN 1533-9211

DOI 10.17605/OSF.IO/HMJBN

Figure 1: U-Net Architecture

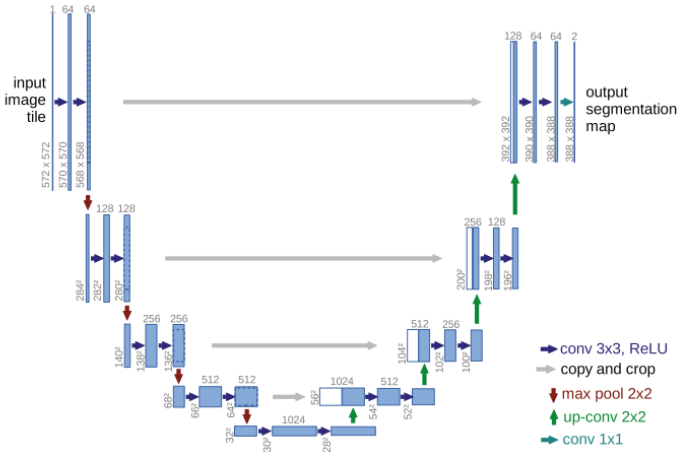

The structural representation of the U-Net architecture consisting of two important parts (encoder and decoder) is shown in Figure 1. Both architectures consist of a convolution layer as a contracting path. The encoder is used for downsampling the image while also increasing the resolution. Meanwhile, the decoder is an expanding path consisting of upsampling operations. In the U-Net architecture, the low-resolution features of the contract path are combined with the enhanced output of the expanding path.

In detecting convective cloud, the present study uses Himawari-8 satellite image data and other supporting data collected in 2021 with the following criteria:

1. Himawari-8 satellite data IR-1 channel in .pgm (Portable Gray Map) and .cn format with a resolution of 0.04° x 0.04° per hour downloaded from the GMS/GOES9/MTSAT Data Archive for Research and Education webpage at http://weather.is.kochi-u.ac.jp/archive-e.html
2. Hourly and daily rainfall observation data from weather observation stations and BMKG rainfall measurement posts in the Medan City area.
3. Upper air observation data (Radiosonde) from the Kualanamu Meteorological Station.

Data processing in this study was done through the following procedures:

1. Meso-scale heavy rains: daily rainfall data from the BMKG Weather Observation Station for the North Sumatra region from 2019 to 2021 was utilized to see mesoscale heavy rain events in the Medan City area. The time of heavy rain occurring evenly at two weather observation stations in the Medan area was chosen as a case study.
2. Pre-processing of cloud image data in .cn format was converted into image data in .TIFF format for easy processing by CC-Unet model.

The employed data were processed through a general approach and deep learning.

ISSN 1533-9211

DOI 10.17605/OSF.IO/HMJBN

Figure 2: Research Flow Chart (yellow color marks the model optimization)

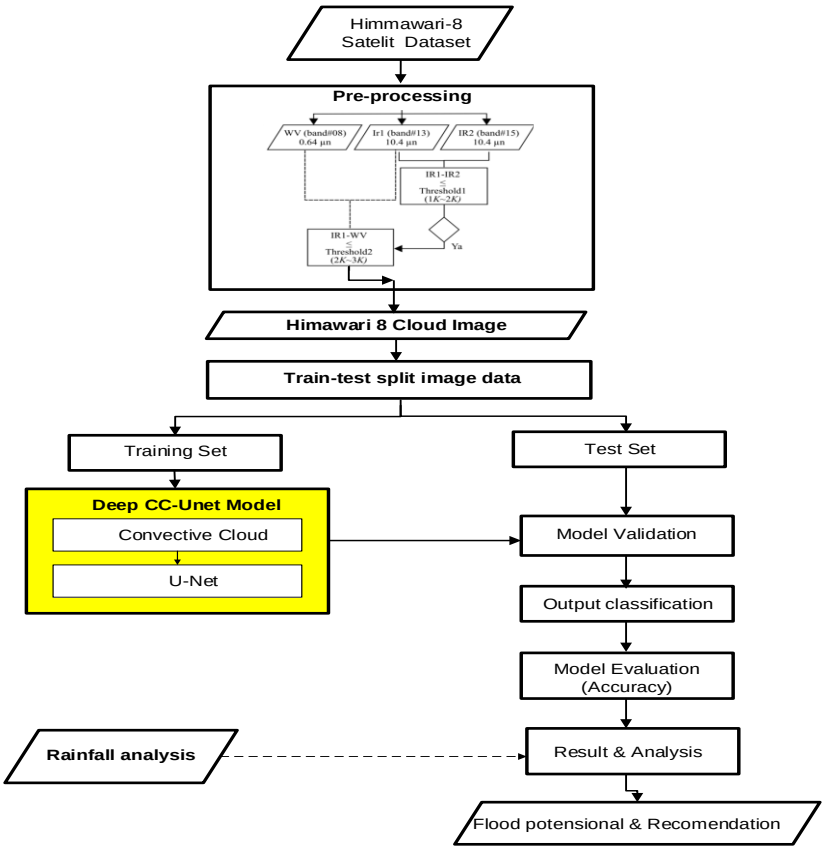

2.4 CC-UNET Architecture Cloud Image Segmentation

The CC-Unet architecture applied to the convection cloud image segmentation is described in Figure 3.

Figure 3: CC-Unet Model

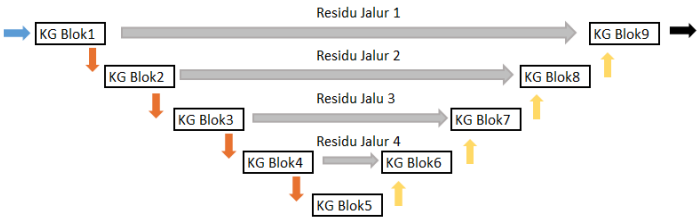

Annotation:

- 3×3 Conv (ReLU)
- 2×2 Max Pooling
- 2×2 Transposed Conv
- 1×1 Conv (Sigmoid)

ISSN 1533-9211

DOI 10.17605/OSF.IO/HMJBN

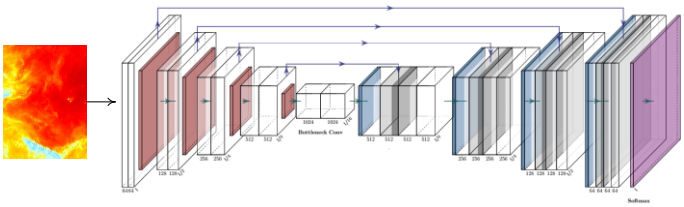

The CC-Unet model above is represented as a layered architecture divided into encoder and decoder (Figure 3). The encoder section performs the downsampling function to reduce the image size consisting of the number of channel (n) parameters; with n= {64, 128, 256, 512}, and activation function (f)= ReLu (Rectified Linear Unit). Meanwhile, the decoder section performs the upsampling function to restore the image size, consisting of the number of channel parameters (n); n= {512, 256, 128, 64}, and the activation function parameter (f)= ReLu. The last part is the output layer as a classified or segmented cloud image. Later, the output parameter is the number of output channels (N), = 1x1, with activation function (f) = Softmax.

Mathematically, the CC-Unet model in Figure 3 can be modeled as equation (6), where convective cloud images were converted into a vector or tensor-based prediction image.

$$f(i) = \sigma\left(\sum_{j=1}^{H_2} u_j, i^{\sigma}\left(\sum_{k=1}^{H_1} u_k, j^{\sigma}\left(\sum_{m=1}^{M} x_m w_{m,k} + \beta_k\right) + \gamma_j\right) + \lambda_i\right) \ldots\ldots\ldots\ldots (6)$$

Where:

β_k, γ_j, and λ_i: the image bias or noise factor.

N: the number of layers.

H: the hidden layer.

M: the final or output layer.

k: the number of image labels or classes.

Determination of the pixel position of the output image on CC-Unet used probability theory. The probability value was calculated using the Softmax function to obtain the right value and produce good segmentation accuracy. The Softmax is described in equation (7) as follows:

$$p_k(x) = exp\left(a_k(x)\right) / \left(\sum_{k'=1}^{K} \exp(a_{k'}(x))\right) \ldots\ldots\ldots\ldots\ldots (7)$$

Where:

p_k: the probability value of pixel x placement in the predicted image. The proposed model for the CC-U-Net architecture appearing in an algorithm 1 is explained through the following stages:

Algorithm 1: CC-Unet-Convective cloud image classification

input: nxm dimension cloud image

for k = 1 to 9 do **:**

The Seybold REPORT
ISSN 1533-9211
DOI 10.17605/OSF.IO/HMJBN

{Step 1 **Encoder line(n)**

c_k = Convolution2D(number of channels**,** (3**,** 3**),** f**)**

c_k = Dropout**(**0.2**)(**c_k**)** //0.2 == weight factor

c_k = Convolution2D **(**64**,** (3**,** 3**),** f**)**

p_k = MaxPooling2D**((**2**,** 2**))(**c_k**)**

{Step 2**: Cloud image decoder (n)**

UK = Conv2DTranspose**(**512**,** (2**,** 2**)(CK-**1**)**

UK = concatenate**([**u_k**,** c_k-2**])**

CK = Conv2D**(**256**,** (3**,** 3**),**f**)(UK)**

CK = Dropout**(**0.2**)(CK)**

CK = Conv2D**(**128**,** (3**,** 3**),** f**)(CK)**

CK = Dropout**(**0.2**)(CK)**

CK = Conv2D**(**64**,** (3**,** 3**),** f**)(CK)**

{Step 3**: Output**

Softmax:

$$\boldsymbol{p}_i(\boldsymbol{x}) = \boldsymbol{exp}\big(\boldsymbol{a}_i(\boldsymbol{x})\big) / (\textstyle\sum_{i'=1}^{K} \boldsymbol{exp}(\boldsymbol{a}_{i'}(\boldsymbol{x})))$$

}

Output:

O_net = Conv2D**(**N**,** dimension, activation**)(CK)**

The two types of activation functions applied in this research were ReLu and Softmax. In the CC-Unet architecture above, the ReLu activation function was applied to each convolution layer. The mathematical function of ReLu is described in equation 8, while Figure 4 is the graph of the ReLu function.

$$ReLu(x) = max(0, x) \quad \ldots\ldots\ldots\ldots(8)$$

$$ReLu\ (x) = \begin{cases} 1 \ if\ x>0 \\ 0 \ if\ x\leq 0 \end{cases}$$

ISSN 1533-9211

DOI 10.17605/OSF.IO/HMJBN

Figure 4: ReLu Function Form

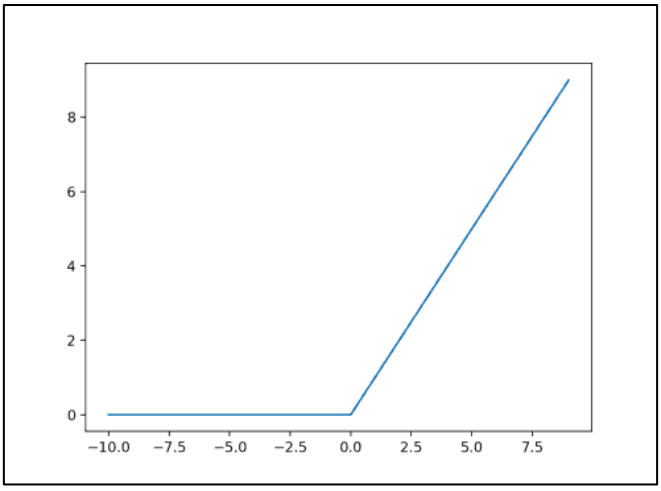

The Softmax activation function was applied to the output layer in the CC-Unit architecture above with equation 9 and was illustrated in algorithm 2.

$$p_k(x) = \exp\left(a_k(x)\right) / \left(\sum_{k'=1}^{K} \exp(a_{k'}(x))\right) \ldots\ldots\ldots\ldots\ldots(9)$$

Where:

$a_k(x)$: an activation function in the k channel at the pixel x position.

K parameter: the number of classes and functions.

$p_k(x)$: the maximum approximation of the function.

Algorithm 2**:** Softmax

Input**:** Image tensor **(**i**)**

Output**:** Tensor, the transformation output of the softmax function is non-negative with a total =1

for i=1,2,3.... do

Calculate the value of e on through the equation: $e = \exp(a_k(i))$

endfor

for j=1,2,3... do

Calculate the value of s through the equation:

$$s = \exp(a_{k'}(i))$$

endfor

output: p(i) =e/s

The Seybold REPORT
ISSN 1533-9211
DOI 10.17605/OSF.IO/HMJBN

Furthermore, the entropy value becomes the final determinant for evaluating the pixel position, as determined with equation (10).

$$E = \sum_{x \in \Omega} w(x) \log(p_{l(x)}(x)) \ldots\ldots\ldots\ldots\ldots(10)$$

Where:

Ω: consists of {1, …., K} a true image label at the time of segmentation.

w: a weight that determines the importance of an image.

2.5 CC-UNIT Model Performance Measurement

The performance of the CC-Unet model was measured quantitatively and qualitatively. The prediction accuracy value evaluated according to the Intersection over Union (IoU) value was a quantitative parameter, as described in equations (11) and (12) below:

$$IoU = \frac{\text{Intersection}}{\text{Union}} \ldots\ldots\ldots\ldots\ldots\ldots (11)$$

$$IoU = \frac{TP}{TP+FP+FN} \ldots\ldots\ldots\ldots\ldots\ldots\ldots..(12)$$

Based on equations (11) and (12) above, True Positive (TP), False Positive (FP), and False Negative (FN) were the sum of the number of image pixels (x) that are correctly, incorrectly, and externally classified as x.

2.6 Cross-Validation

Since Cross-Validation (CV) is generally used to test the performance of the model, D image data in this study were randomly divided into k-subsets of data $D_1, D_2, D_3 \ldots D_k$ with the same size between sub-sets of data using the k-Fold cross-validation method.

3. RESULTS AND DISCUSSIONS

3.1 Econometrics Cointegration

The Augmented Dickey-Fuller unit root test by adopting the Dickey & Fuller (1979) method was done for checking the data stationarity. The unit root test results are presented in Table 1:

Table 1: Unit root test results

Variable	t-statistics	Stationary level	Prob.*
Gross Regional Domestic Product (GRDP)	-3.175352	Level/I(0)	0.0076
Human Development Index (HDI)	-3.212696	Level/I(0)	0.0052
Poverty (POV)	-3.259808	1st difference	0.0022
Aquaculture Production (AP)	-3.212696	Level/I(0)	0.0005

*denotes the significance in 5% level.

The unit-root test using the Augmented Dickey-Fuller (1979) found no variable was integrated into the second order/I(2), emphasizing that the present data was not spurious but eligible to

The Seybold REPORT
ISSN 1533-9211
DOI 10.17605/OSF.IO/HMJBN

run in the model. In finding the cointegration that also defines the causal relationship through the ARDL model, it is necessary to determine the optimum lag of all variables as a group. Because the nature of the data in this study is annual, lag-1 to lag-2 is highly recommended. According to Dickey & Fuller (1979), too high of lag can lead the model to lose degrees of freedom, cause multicollinearity, and generate serial correlation problems. Optimum Lag results through VAR Estimates Lag Order are presented in Table 2:

Table 2: A Vector Autoregressive Lag Order

Lag	LogL	LR	FPE	AIC	SC	HQ
0	58.59727	N/A	5.756101	-9.926777	-9.782088	-10.01798
1	106.4935	52.25040*	2.322032*	-15.72609*	-15.00264*	-11.18212*

*indicates lag order selected by the criterion

LR: sequential modified LR test statistic (each test at 5% level)

FPE: Final Prediction Error

AIC: Akaike Information Criterion

SC: Schwarz Information Criterion

HQ: Hannan-Quinn Information Criterion

The optimum lag marked with an asterisk is indicated as the best lag for the model (the lag with the smallest value). Therefore, this study had to use the Akaike Information Criterion (AIC lag 1) and entered them into the model when running ARDL Cointegrating and Long Run Forms to look for long-term cointegration. Cointegrating and Long Run Form results are presented in Table 3 below:

Table 3: ARDL Cointegrating and Long Run Form

Dependent variable	CointEq(-1)
GRDP	0.1724
HDI	0.0931
POV	0.0383
AP	0.6327

When the poverty parameter as a determiner of whether or not societies are able to meet their basic needs was set as the dependent variable, long-term co-integration was found with a significance level of 5%. For testing it further, a Bound Test was carried out with the results presented in Table 4 below:

Table 4: ARDL Bounds Test

Dependent variable	F-statistic
POV	26.78748

The F-statistic of POV from the ARDL Bounds Test was 26.78748. As suggested by Pesaran et al., (2001), cointegration was found if the F-Statistics from the ARDL Bounds Test was greater than the upper critical bound (UCB). Therefore, the poverty variable in this study has

ISSN 1533-9211

DOI 10.17605/OSF.IO/HMJBN

long-run cointegration as its F-statistic was higher than UCB at the 5% level (4.35), as shown in Table 5 below:

Table 5: Critical Value Bounds

Significance	LCB	UCB
10%	2.72	3.77
5%	3.23	4.35
2.50%	3.69	4.89
1%	4.29	5.61

LCB: Lower critical bound
UCB: Upper critical bound

Poverty as the dependent variable proved to have long-term cointegration with some variables. Therefore, the VECM test must be continued with POV as the endogenous variable. The VECM test results are presented in Table 6:

Table 6: Vector Error Correction Model Test Results for POV

Variable	Coefficient	Std. Error	t-Statistic	Prob.
GRDP	-0.094561	0.817079	0.139077	0.00183
HDI	0.046319	0.13443)	0.59429	0.06944
AP	-0.817079	0.38281	0.15912	0.00567
C	7.72805	2.15173	5.32141	0.41859

The results from the Vector Error Correction Model Test Results for POV proved that long-term cointegration was found with two variables. As shown in Table 6, the prob values of the AP and GRDP variables are significant ($\alpha<0.05$) as much as the coefficients given when POV was used as the dependent variable. Therefore, if the Medan City government can increase GRDP and AP by 1% each, POV can be reduced by 0.094561% and 0.817079% respectively.

3.2 The Convolution Neural Network

This study aims to improve the accuracy performance of the CC-Unet model from other types of methods such as Segnet. Figure 5 below is the conversion result of the original satellite image in .cn to .TIFF format which was carried out in the pre-processing stage.

Figure 5: The Results of the Himawari-8 Satellite Cloud Image Plot

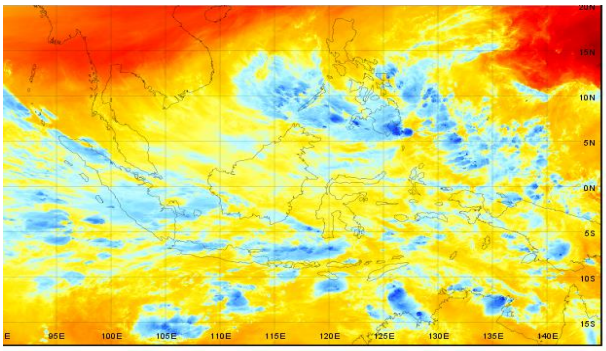

ISSN 1533-9211

DOI 10.17605/OSF.IO/HMJBN

3.3 Test Results With The CC-Net Model

In the concept of deep learning, the loss value must be minimized by the Sara network because this value is useful to describe the difference between the actual and predicted labels (Lecun et al., 2015). Therefore, the neural network learns to adjust the weights and bias values until they reach a minimum value by minimizing losses.

The performance graph of the CC-Unet model with epoch values of 50 iterations is presented in Figures 6 and 7.

Figure 6: Loss Graph of the CC-Unet Model

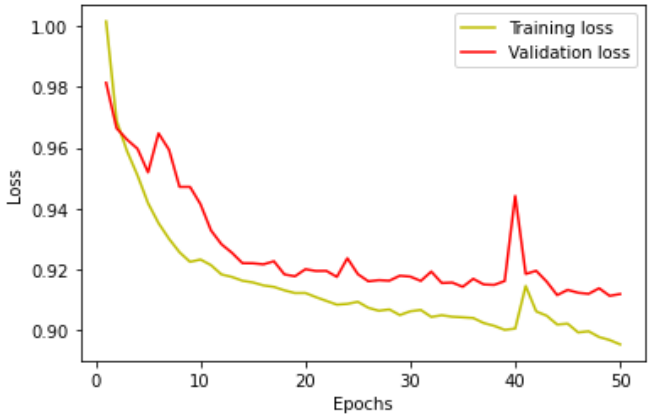

Figure 7: Accuracy Graph of the CC-Unet Model

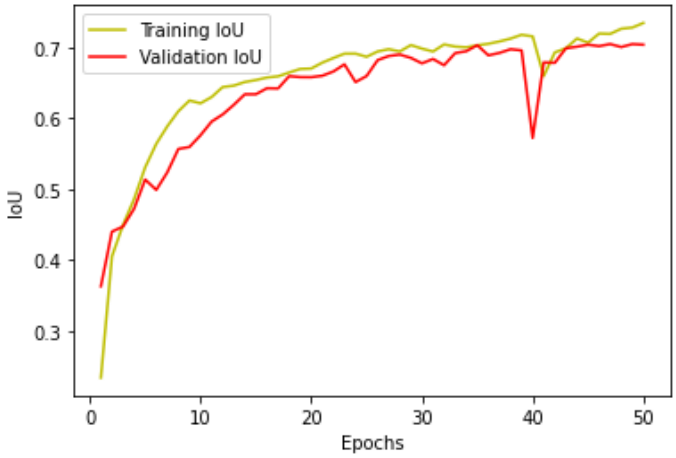

In Figure 6, the loss value during the training and model testing decreases as the training data increases. On the other hand, the accuracy during the model training and testing continued to increase with increasing epochs as shown in Figure 7.

The performance of the CC-Unet model compared to its predecessor model (U-net) based on the classification of convective cloud images in this study is presented in Table 7 below:

ISSN 1533-9211

DOI 10.17605/OSF.IO/HMJBN

Table 7: Comparison of Accuracy

CC-Unet	U-net
92.32	87.37
97.05	91.37
98.22	96.37
97.45	94.37
97.67	95.37
98.17	95.37
96.20	93.37
98.70	96.37
98.77	97.37
98.34	94.37
97.29	94.17

The average accuracy of the U-Net and CC-Unet models in the performance test was carried out in 10 batches by monitoring the performance accuracy. Respectively, CC-Unet and U-Net have an average accuracy of 97.29% and 94.17%. As a U-Net-based model, the test results of the CC-Unet model in classifying Himawari-8 satellite imagery are presented in Figure 8 below.

Figure 8: Result Comparisons of U-Net Accuracy toward the CC-Unet Model

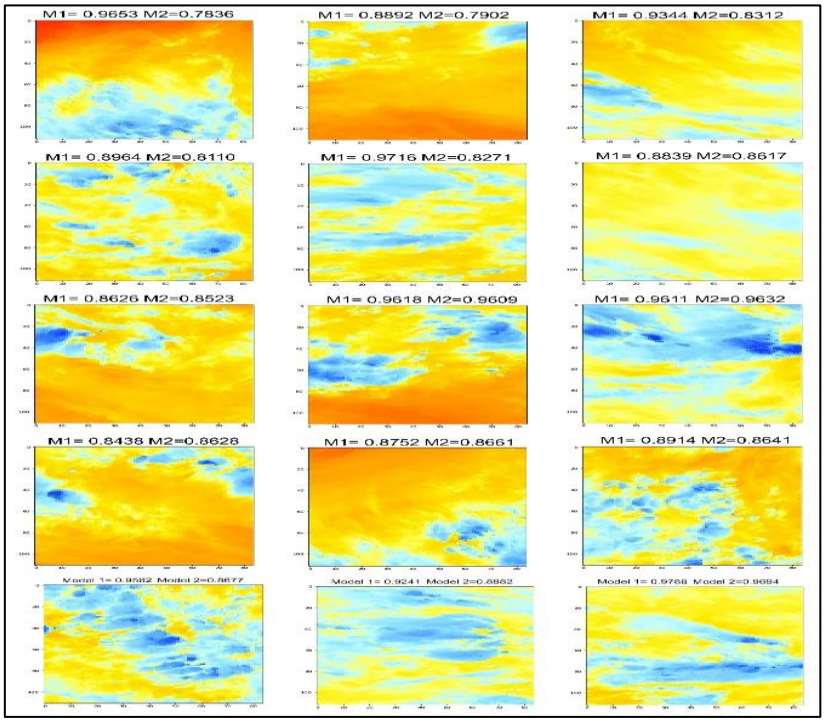

ISSN 1533-9211

DOI 10.17605/OSF.IO/HMJBN

3.4 Model Significance Test

Statistical significance using the Wilcoxon test was used to test whether the results of the model performance in Figure 2 were significant at the 95% level. The Wilcoxon test was declared to be significantly different with the assumption that the p-value < 0.05, as presented in Table 8.

Table 8: The results of the Wilcoxon test for the CC-Unet model

VS	R^+	R^-	Exact P-value	Asymptotic P-value
U-Net	112.0	8.0	0.0015258	0.002866

In Table 8, the p-value of the U-Net model is 0.0015258 < 0.05 which indicates that the accuracy of CC-Unet is significantly different from the results of Refined U-net.

Figure 9: Convective cloud image segmentation results

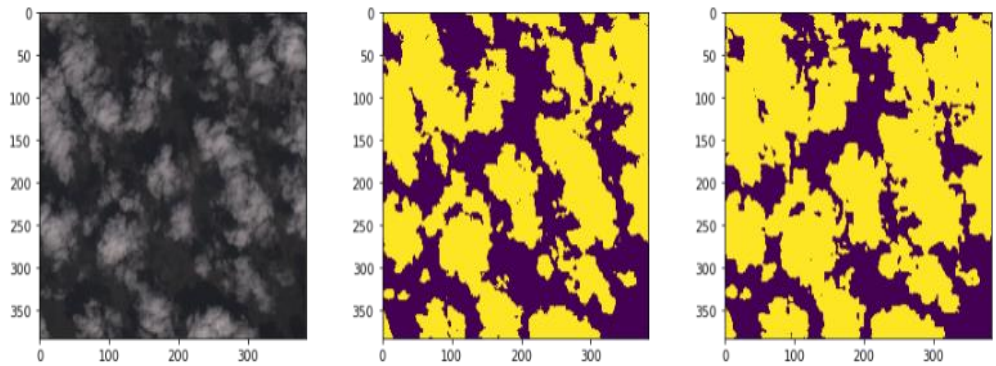

a. Original image b. Ground truth image c. Predicted image

For determining whether the predicted images were truly segmented, then the level of similarity of the ground truth to the predicted images was tested. The result of the similarity test based on the root mean square error (rmse) between the ground truth image and the predicted image was 0.0218. Since the rmse value obtained was very small, the similarity between the images is high.

3.5 Model Verification And Validation Results

Based on the extreme weather events that occurred on October 30, 2021, as forewarned by the Indonesian Meteorology, Climatology and Geophysics Agency, the community in the Aur Village area of Medan was hit by significant flooding on October 30-31, 2021. The flood height caused by extreme weather at that time reached one meter, and the worst point was witnessed in Aur Village, precisely on the banks of the Deli River (Info Indonesia, 2021).

Visually, the classification results of convective cloud images show that the CC-Unet model can exhibit convective cloud images that are close to the Himawari-8 satellite image. Therefore, it is hoped that the verification and validation of convective cloud images with the CC-Unet model can be used to predict rainfall and provide early flood warnings in Medan City better and more accurately.

ISSN 1533-9211

DOI 10.17605/OSF.IO/HMJBN

Figure 10: Himawari-8 satellite image and validation results of rain predictions in Medan City using the CC-Unet model

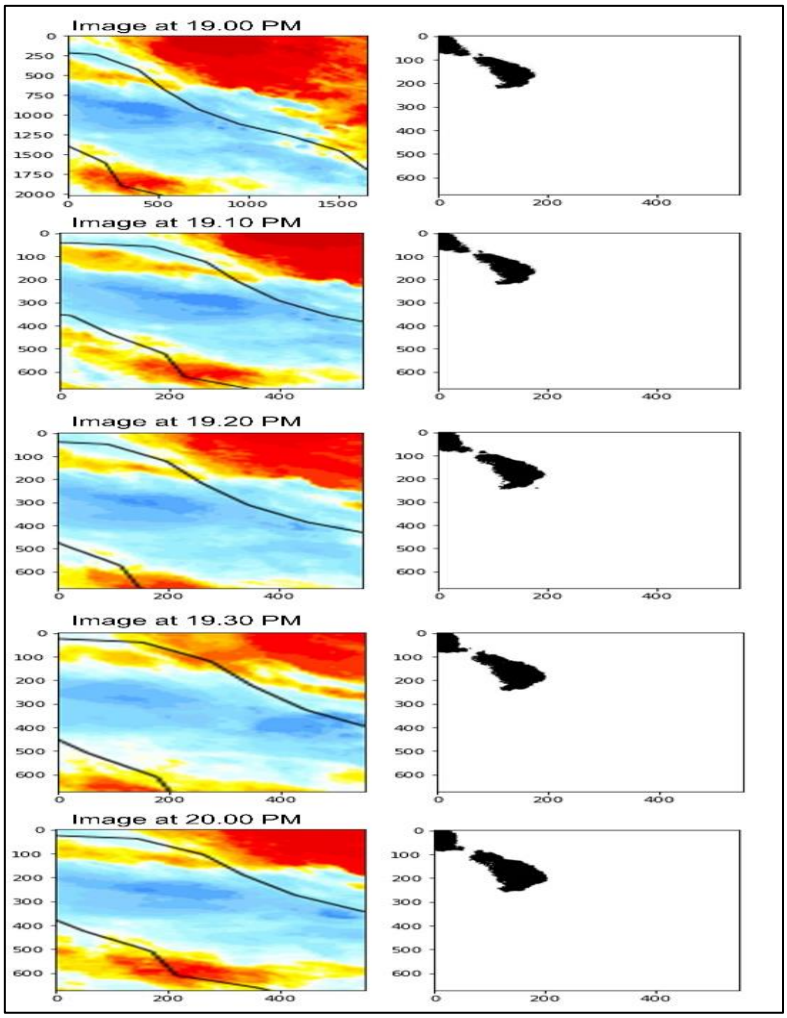

Flooding, one of the disasters with the highest level of impact on all mankind (Posthumus et al., 2008; Surminski & Eldridge, 2017), is becoming more extreme due to climate change (Conway et al., 2010). According to Ahmed et al., (2019), high and unpredictable rainfall causes the floods frequency to become more dangerous with large volumes. Due to their intensity, floods always cause damage to aquaculture infrastructure. Furthermore, when it happens over a prolonged period, the destruction gets super destructive.

The prospect of aquaculture production is extremely vulnerable to environmental problems because aquaculture businesses always face various threats such as cyclone storms, variations in rainfall, global warming, and rising sea levels, which in turn cause flooding (Brander, 2007; De Silva & Soto, 2009; Ahmed & Diana, 2015). The hazard of climate change according to Kwiatkowski et al., (2017) will have a severe impact on aquaculture production, where global fisheries production is predicted to decrease by 6% in 2100. In line with these findings, the

The Seybold REPORT
ISSN 1533-9211
DOI 10.17605/OSF.IO/HMJBN

frequency of flooding due to cyclonic storms and global warming according to Vitousek et al., (2017) will experience a two-fold increase in severity by 2050 due to a sea level rise of 10-20 cm in some areas with limited water level variability, particularly in tropical countries.

Several studies (Béné et al., 2007; Heck et al., 2007), confirmed that the fisheries sector has an immense contribution to reducing poverty levels. Furthermore, the World Bank (2012) stated that if the aquaculture sector was managed and utilized as productively as possible, one country can gain massive benefits to improve the standard of living of the aquaculture community. Unfortunately, floods often cause losses to shrimp farming due to decreased water quality, such as sediment brought on by erosion, intrusion of water with over-tolerance salinity, and other types of pollution brought by the floods. Losses due to floods will have a direct impact on total production which affects the GRDP level. Molle et al., (2010) stated that the aquaculture sector is vulnerable to floods. When a flood occurs, the possibility of contamination being spread against the aquaculture business is very likely to occur. The study by Fahmi et al., (2022) in Langkat Regency, North Sumatra, found that flooding had caused major losses to aquaculture activities. They found that when the tide coincided with the rainy season, the cultivation ponds became unable to accommodate the water discharge and pollution causing them to have lost around IDR 100 million. In line with these findings, vannamei shrimp cultivators have also experienced floods in Brebes (Suripto, 2022), Pati (Aji, 2020), and in the Mekong Delta in Vietnam (Nguyen et al., 2014) with losses of up to hundreds of millions.

The results from the Vector Error Correction Model Test Results for the poverty variable proved that long-term cointegration was found with two other variables. As shown in Table 6, the probability values of the AP and GRDP variables are significant ($\alpha<0.05$) as much as the coefficients given when the poverty variable was used as the dependent variable. Therefore, if the Medan City government can increase GRDP and aquaculture production by around 1% each by anticipating loss due to environmental damage such as floods, poverty can be reduced by 0.094561% and 0.817079% respectively.

Given that the aquaculture sector has a crucial role in supplying the needs of global fisheries demand (Troell et al., 2009; Beveridge et al., 2013), it is necessary to carry out wise steps through flood disaster mitigation as early as possible. Local governments should consider protecting the aquaculture sector from disaster since floods will harm the total production operated by shrimp cultivators. Studies by Ali & Rehman (2015), found that low income will likely affect societies and continuously influence the GRDP. Therefore, when the aquaculture sector is protected from flood disasters, income and production capacity will be more heightened. Accordingly, when income is high, the capital gained by the cultivators can encourage economic growth wholesomely.

It is hoped that predictions regarding the occurrence of clouds that cause flooding can be well constructed. Once the application is widely adopted, it is easier for all parties to understand the threat of flooding that might occur in the future. The prediction of flooding can be used by shrimp farming business actors in Medan City, especially Aur Village, for preventing losses against their shrimp production.

The Seybold REPORT
ISSN 1533-9211
DOI 10.17605/OSF.IO/HMJBN

4. CONCLUSIONS AND SUGGESTIONS

Poverty variable proved to have long-term cointegration with the aquaculture production and Gross Regional Domestic Product variables in Medan City. If the local government in Medan City can increase GRDP and aquaculture production at 1% each by protecting the aquaculture sector from disaster since floods will harm the aquaculture production operated by shrimp cultivators, poverty can be reduced by 0.094561% and 0.817079% respectively.

The CC-Unet model in this study has a better accuracy of 97.29% compared to the U-Net model (94.17%). Therefore, the accuracy of CC-Unet between the ground truth image and the predicted image was very close. Since CC-Unet has proven to be one of the models in deep neural network (DNN) which has been successfully used to predict heavy rain based on the classification of convective cloud imagery, the CC-Unet model is expected to be broadly employed in predicting rainfall and providing a more reliable flood early warning in Medan City. Once the application is widely adopted, it is easier for all parties to understand the threat of flooding that might occur in the future. The prediction of flooding can be used by shrimp farming business actors in Medan City, especially Aur Village, for preventing losses against their shrimp production.

5. ACKNOWLEDGEMENTS

We thank our colleagues at the Faculty of Computer Science and Information Technology, University of North Sumatra, for the collaborative contribution to the success of this research.

Disclosure Statement

The authors declare that there is no conflict of interest.

References

- Ackerman, S. A., Strabala, K. I., Menzel, W. P., Frey, R. A., Moeller, C. C., & Gumley, L. E. (1998). Discriminating clear sky from clouds with MODIS. Journal of Geophysical Research, 103(D24), 32141-32157. https://doi.org/10.1029/1998jd200032
- Ahmed, N., & Diana, J. S. (2015). Threatening “white gold”: impacts of climate change on shrimp farming in coastal Bangladesh. Ocean & Coastal Management, 114 (2015), 42-52. https://doi.org/10.1016/j.ocecoaman.2015.06.008
- Ahmed, N., Thompson, S., & Glaser, M. (2019). Global aquaculture productivity, environmental sustainability, and climate change adaptability. Environmental Management, 63(2), 159-172. https://doi.org/10.1007/s00267-018-1117-3
- Aji, D. U. (July, 15, 2022). Petani tambak di Margoyoso Pati rugi ratusan juta akibat banjir bandang. Detik News. Accessed on 02 September 2022. Retrieved from https://www.detik.com/jateng/berita/d-6181739/petani-tambak-di-margoyoso-pati-rugi-ratusan-juta-akibat-banjir-bandang
- Ali, A., & Rehman, H. U. (2015). Macroeconomic instability and its impact on gross domestic product: an empirical analysis of Pakistan. Pakistan Economic and Social Review, 53(2), 285-316. Retrieved from https://www.jstor.org/stable/26153261

The Seybold REPORT
ISSN 1533-9211
DOI 10.17605/OSF.IO/HMJBN

- Anbumozhi, V., Matsumoto, K., & Yamaji, E. (2001). Sustaining agriculture through modernizing of irrigation tanks: an opportunities and challenge for Tamil Nadu. Agricultural Engineering International: CIGR Journal of Scientific Research and Development, 1(2), 1-12. Retrieved from https://ecommons.cornell.edu/bitstream/handle/1813/10239/LW%2001%20002.pdf?sequence=1&isAllowed=y
- Badrinarayanan, V., Kendall, A., & Cipolla, R. (2017). SegNet: a deep convolutional encoder-decoder architecture for image segmentation. IEEE Transactions on Pattern Analysis and Machine Intelligence, 39(12), 2481–2495. https://doi.org/10.1109/TPAMI.2016.2644615
- Bai, T., Li, D., Sun, K., Chen, Y., & Li, W. (2016). Cloud detection for high-resolution satellite imagery using machine learning and multi-feature fusion. Remote Sensing, 8(9), 1-21. https://doi.org/10.3390/rs8090715
- Baker, M. B., & Peter, T. (2008). Small-scale cloud processes and climate. Nature, 451(7176), 299-300. https://doi.org/10.1038/nature06594
- Baum, B. A., Menzel, W. P., Frey, R. A., Tobin, D. C., Holz, R. E., Ackerman, S. A., Heidinger A. K., & Yang, P. (2012). MODIS cloud-top property refinements for collection 6. Journal of Applied Meteorology and Climatology, 51(6), 1145-1163. https://doi.org/10.1175/jamc-d-11-0203.1
- Béné, C., Macfayden, G., & Allison, E. H. (2007). Increasing the contribution of small-scale fisheries to poverty alleviation and food security. FAO Fisheries Technical Paper. Food and Agriculture Organization of the United Nations (FAO), Rome, Italy. http:// dx.doi.org/10.1017/CBO9781107415324.004. Retrieved from http://www.fao.org/docrep/009/ a0965e/a0965e00.HTM.
- Bessho, K., Date, K., Hayashi, M., Ikeda, A., Imai, T., Inoue, H., Kumagai, Y., Miyakawa, T., Murata, H., Ohno, T., Okuyama, A., Oyama, R., Sasaki, Y., Shimazu, Y., Shimoji, K., Sumida, Y., Suzuki, M., Taniguchi, H., Tsuchiyama, H., Uesawa, D., Yokota, H., & Yoshida, R. (2016). An introduction to Himawari-8/9-Japan's new-generation geostationary meteorological satellites. Journal of the Meteorological Society of Japan. Ser. II, 94(2), 151-183. https://doi.org/10.2151/jmsj.2016-009
- Beveridge, M. C., Thilsted, S. H., Phillips, M. J., Metian, M., Troell, M., & Hall, S. J. (2013). Meeting the food and nutrition needs of the poor: the role of fish and the opportunities and challenges emerging from the rise of aquaculture. Journal of Fish Biology, 83(4), 1067-1084. https://doi.org/10.1111/jfb.12187
- Brander, K. M. (2007). Global fish production and climate change. Proceedings of the National Academy of Sciences, 104(50), 19709-19714. https://doi.org/10.1073/pnas.0702059104
- Chen, N., Li, W., Gatebe, C., Tanikawa, T., Hori, M., Shimada, R., Aoki, T., & Stamnes, K. (2018). New neural network cloud mask algorithm based on radiative transfer simulations. Remote Sensing of Environment, 219(2018), 62-71. https://doi.org/10.1016/j.rse.2018.09.029
- Conway, G., Waage, J., & Delaney, S. (2010). Science and innovation for development. London: UK Collaborative on Development Sciences.
- De Silva, S. S., & Soto, D. (2009). Climate change and aquaculture: potential impacts, adaptation and mitigation. Climate change implications for fisheries and aquaculture: overview of current scientific knowledge. FAO Fisheries and Aquaculture Technical Paper, 530(2009), 151-212.

The Seybold REPORT
ISSN 1533-9211
DOI 10.17605/OSF.IO/HMJBN

- Dickey, D. A., & Fuller, W. A. (1979). Distribution of the estimators for autoregressive time series with a unit root. Journal of the American Statistical Association, 74(366), 427-431.
- Fahmi, M., Harahap, R. U., Dara, R. R., Siregar, H., & Arifin, S. B. (2022). Meningkatkan produktivitas budidaya udang Vaname di Kabupaten Langkat Kecamatan Besitang Provinsi Sumatera Utara. Pubarama: Jurnal Publikasi Pengabdian Kepada Masyarakat, 2(4), 1-8. Accessed on 02 September 2022. Retrieved from http://www.jurnalpkmibbi.org/index.php/Pubarama/article/view/66
- Frey, R. A., Ackerman, S. A., Liu, Y., Strabala, K. I., Zhang, H., Key, J. R., & Wang, X. (2008). Cloud detection with MODIS. Part I: improvements in the MODIS cloud mask for collection 5. Journal of Atmospheric and Oceanic Technology, 25(7), 1057–1072. https://doi.org/10.1175/2008jtecha1052.1
- Gomis-Cebolla, J., Jimenez, J. C., & Sobrino, J. A. (2020). MODIS probabilistic cloud masking over the Amazonian evergreen tropical forests: a comparison of machine learning-based methods. International Journal of Remote Sensing, 11(1), 185–210. https://doi.org/10.1080/01431161.2019.1637963
- Guo, Y., Liu, Y., Georgiou, T., & Lew, M. S. (2018). A review of semantic segmentation using deep neural networks. International Journal of Multimedia Information Retrieval, 7(2), 87-93. https://doi.org/10.1007/s13735-017-0141-z
- Hao, S., Zhou, Y., & Guo, Y. (2020). A brief survey on semantic segmentation with deep learning. Neurocomputing, 406(2020), 302-321. https://doi.org/10.1016/J.NEUCOM.2019.11.118
- Harisdani, D. D., & Lindarto, D. (2018). Partisipasi masyarakat dalam penggunaan teknik biopori untuk mengendalikan banjir kota (studi kasus: Kelurahan Tanjung Rejo-Medan). NALARs, 17(2), 97-104. https://doi.org/10.24853/nalars.17.2.97-104 [in Indonesian]
- Harvey, B. C. (1987). Susceptibility of young of the year fishes to downstream displacement by flooding. Transactions of the American Fisheries Society, 116(6), 851-855. https://doi.org/10.1577/1548-8659(1987)116%3C851:SOYFTD%3E2.0.CO;2
- Heck, S., Béné, C., & Reyes-Gaskin, R. (2007). Investing in African fisheries: building links to the Millennium Development Goals. Fish and Fisheries, 8(3), 211-226. https://doi.org/10.1111/j.1467-2679.2007.00251.x
- Hu, K., Zhang, D., & Xia, M. (2021). Cdunet: cloud detection unet for remote sensing imagery. Remote Sensing, 13(22), 1–22. https://doi.org/10.3390/rs13224533
- Info Indonesia. (October 20, 2021). Imbauan BMKG: waspada hujan berpotensi banjir di Sumut. Info Indonesia. Accessed on 02 September 2022. Retrieved from https://www.infoindonesia.id/read/2021/10/20/8647/imbauan-bmkg:-waspada-hujan-berpotensi-banjir-di-sumut
- Ito, M., & Ino, F. (2018). An automated method for generating training sets for deep learning based image registration. BIOIMAGING 2018-5th International Conference on Bioimaging, Proceedings; Part of 11th International Joint Conference on Biomedical Engineering Systems and Technologies, 2018(2), 140–147. https://doi.org/10.5220/0006634501400147
- Jiao, L., Huo, L., Hu, C., & Tang, P. (2020). Refined UNet: UNet-based refinement network for cloud and shadow precise segmentation. Remote Sensing, 12(12): 1–28. https://doi.org/10.3390/rs12122001

- Kollias, C., Naxakisb, C., & Zarangasb, L. (2004). Defence spending and growth in Cyprus: a causal analysis. Defence and Peace Economics, 15(3), 299-307. https://doi.org/10.1080/1024269032000166864
- Kong, Y., Ma, X., & Wen, C. (2022). A new method of deep convolutional neural network image classification based on knowledge transfer in small label sample environment. Sensors, 22(3), 1-16. https://doi.org/10.3390/s22030898
- Kwiatkowski, L., Bopp, L., Aumont, O., Ciais, P., Cox, P. M., Laufkötter C., Li Y., & Séférian R. (2017). Emergent constraints on projections of declining primary production in the tropical oceans. Nature Climate Change, 7(5), 355-358. https://doi.org/10.1038/nclimate3265
- Lecun, Y., Bengio, Y., & Hinton, G. (2015). Deep learning. Nature, 521(7553), 436-444. https://doi.org/10.1038/NATURE14539
- Liu, C., Yang, S., Di, D., Yang, Y., Zhou, C., Hu, X., & Sohn, B. J. (2021). A machine learning-based cloud detection algorithm for the Himawari-8 spectral image. Advances in Atmospheric Sciences, 39(2021), 1-14. https://doi.org/10.1007/S00376-021-0366-X
- Liu, X., Du, H., Xu, J., & Qiu, B. (2022). DBGAN: A dual-branch generative adversarial network for undersampled MRI reconstruction. Magnetic Resonance Imaging, 89(2011), 77–91. https://doi.org/https://doi.org/10.1016/j.mri.2022.03.003
- Lou, A., Guan, S., & Loew, M. H. (2021). DC-UNet: rethinking the U-Net architecture with dual channel efficient CNN for medical image segmentation. SPIE Digital Library. Retrieved from https://www.spiedigitallibrary.org/conference-proceedings-of-spie/11596/2582338/DC-UNet--rethinking-the-U-Net-architecture-with-dual/10.1117/12.2582338.short?SSO=1. https://doi.org/10.1117/12.2582338
- Minaee, S., Boykov, Y. Y., Porikli, F., Plaza, A. J., Kehtarnavaz, N., & Terzopoulos, D. (2021). Image segmentation using deep learning: a survey. IEEE Transactions on Pattern Analysis and Machine Intelligence, 44(7), 3523-3542. https://doi.org/10.1109/TPAMI.2021.3059968
- Mohanty, S. P., Czakon, J., Kaczmarek, K. A., Pyskir, A., Tarasiewicz, P., Kunwar, S., Rohrbach, J., Luo, D., Prasad, M., Fleer, S., Göpfert, J. P., Tandon, A., Mollard, G., Rayaprolu, N., Salathe, M., & Schilling, M. (2020). Deep Learning for understanding satellite imagery: an experimental survey. Frontiers in Artificial Intelligence, 3(2020), 85-86. https://doi.org/10.3389/FRAI.2020.534696/BIBTEX
- Molle, F., Wester, P., & Hirsch, P. (2010). River basin closure: Processes, implications and responses. Agricultural Water Management, 97(4), 569-577. https://doi.org/10.1016/j.agwat.2009.01.004
- Mushtaq, S., Dawe, D., & Hafeez, M. (2007). Economic evaluation of small multi-purpose ponds in the Zhanghe irrigation system, China. Agricultural Water Management, 91(1-3), 61-70. DOI: https://doi.org/10.1016/j.agwat.2007.04.006
- Mushtaq, S., Dawe, D., Lin, H., & Moya, P. (2006). An assessment of the role of ponds in the adoption of water-saving irrigation practices in the Zhanghe Irrigation System, China. Agricultural Water Management, 83(1-2), 100-110. https://doi.org/10.1016/j.agwat.2005.10.004
- Nguyen, A. L., Dang, V. H., Bosma, R. H., Verreth, J. A., Leemans, R., & De Silva, S. S. (2014). Simulated impacts of climate change on current farming locations of striped catfish (Pangasianodon hypophthalmus; Sauvage) in the Mekong Delta, Vietnam. AMBIO, 43(8), 1059-1068. https://doi.org/10.1007/s13280-014-0519-6

The Seybold REPORT
ISSN 1533-9211
DOI 10.17605/OSF.IO/HMJBN

- Pan, Z., Xu, J., Guo, Y., Hu, Y., & Wang, G. (2020). Deep learning segmentation and classification for urban village using a worldview satellite image based on U-net. Remote Sensing, 12(10), 1-17. https://doi.org/10.3390/rs12101574
- Pesaran, M. H., Shin, Y., & Smith, R. J. (2001). Bounds testing approaches to the analysis of level relationships. Journal of Applied Econometrics, 16(3), 289-326. https://doi.org/10.1002/jae.616
- Posthumus, H., Hewett, C. J. M., Morris, J., & Quinn, P. F. (2008). Agricultural land use and flood risk management: Engaging with stakeholders in North Yorkshire. Agricultural Water Management, 95(7), 787-798. https://doi.org/10.1016/j.agwat.2008.02.001
- Prabawadhani, D. R., Harsoyo, B., Seto, T. H., & Prayoga, B. R. (2016). Karakteristik temporal dan spasial curah hujan penyebab banjir di wilayah DKI Jakarta dan sekitarnya. Jurnal Sains & Teknologi Modifikasi Cuaca, 17(1), 21-24. https://doi.org/10.29122/jstmc.v17i1.957
- Rahmawati, F. (December 5, 2020). Terparah sejak 20 tahun terakhir, ini 3 fakta banjir di Kampung Lalang Medan. Merdeka News. Accessed on 02 September 2022. Retrieved from https://www.merdeka.com/sumut/terparah-sejak-20-tahun-terakhir-ini-3-fakta-banjir-di-kampung-lalang-medan.html
- Ronneberger, O., Fischer, P., & Brox, T. (2015). U-Net: convolutional networks for biomedical image segmentation BT-medical image computing and computer-assisted intervention-MICCAI 2015. N. Navab, J. Hornegger, W. M. Wells, & A. F. Frangi (eds.). Springer International Publishing. pp. 234–241.
- Sato, T. (2006). Dramatic decline in population abundance of Salvelinus leucomaenis after a severe flood and debris flow in a high gradient stream. Journal of Fish Biology, 69(6), 1849-1854. https://doi.org/10.1111/j.1095-8649.2006.01222.x
- Schlosser, I. J. (1985). Flow regime, juvenile abundance, and the assemblage structure of stream fishes. Ecology, 66(5), 1484-1490. https://doi.org/10.2307/1938011
- She, L., Zhang, H. K., Li, Z., de Leeuw, G., & Huang, B. (2020). Himawari-8 aerosol optical depth (AOD) retrieval using a deep neural network trained using AERONET observations. Remote Sensing, 12(24), 4125-4127. https://doi.org/10.3390/RS12244125
- Suripto, I. (August 09, 2022). Dampak perubahan iklim, udang tambak di Brebes gagal dipanen. Detik News. Accessed on 02 September 2022. Retrieved from https://news.detik.com/berita/d-6224307/dampak-perubahan-iklim-udang-tambak-di brebes-gagal-dipanen.
- Surminski, S., & Eldridge, J. (2017). Flood insurance in England–an assessment of the current and newly proposed insurance scheme in the context of rising flood risk. Journal of Flood Risk Management, 10(4), 415-435. https://doi.org/10.1111/jfr3.12127
- Tarigan, A. K., Samsura, D. A. A., Sagala, S., & Pencawan, A. V. (2017). Medan City: Development and governance under the decentralisation era. Cities, 71(2017), 135-146. https://doi.org/10.1016/j.cities.2017.07.002
- Toth, L. A., Dudley, D. R., Karr, J. R., & Gorman, O. T. (1982). Natural and man-induced variability in a silverjaw minnow (Ericymba buccata) population. American Midland Naturalist, 107(2), 284-293. https://doi.org/10.2307/2425379

The Seybold REPORT
ISSN 1533-9211
DOI 10.17605/OSF.IO/HMJBN

- Troell, M., Joyce, A., Chopin, T., Neori, A., Buschmann, A. H., & Fang, J. G. (2009). Ecological engineering in aquaculture—potential for integrated multi-trophic aquaculture (IMTA) in marine offshore systems. Aquaculture, 297(1-4), 1-9. https://doi.org/10.1016/j.aquaculture.2009.09.010
- Vitousek, S., Barnard, P. L., Fletcher, C. H., Frazer, N., Erikson, L., & Storlazzi, C. D. (2017). Doubling of coastal flooding frequency within decades due to sea-level rise. Scientific Reports, 7(1), 1-9. https://doi.org/10.1038/s41598-017-01362-7
- World Bank. (2012). Hidden Harvest: The Global Contribution of Capture Fisheries. World Bank, Washington, D.C.
- Xie, W., Liu, D., Yang, M., Chen, S., Wang, B., Wang, Z., Xia, Y., Liu, Y., Wang, Y., Zhang, C. (2020). SegCloud: A novel cloud image segmentation model using a deep convolutional neural network for ground-based all-sky-view camera observation. Atmospheric Measurement Techniques, 13(4), 1953-1961. https://doi.org/10.5194/amt-13-1953-2020
- Yu, F., Koltun, V. (2016). Multi-scale context aggregation by dilated convolutions. 4th International Conference on Learning Representations ICLR 2016-Conference Track Proceedings. Retrieved from https://arxiv.org/pdf/1511.07122.pdf https://doi.org/10.48550/arXiv.1511.07122